Performances of a prototype for the ALICE muon trigger at LHC

P. Dupieux

To cite this version:

P. Dupieux. Performances of a prototype for the ALICE muon trigger at LHC. IEEE-NPSS (Nuclear and Plasma Sciences Society) 13, May 2003, Montreal,Quebec, Canada. 2003. <in2p3-00013791>

HAL Id: in2p3-00013791
http://hal.in2p3.fr/in2p3-00013791
Submitted on 3 Jul 2003

Performances of a prototype for the ALICE muon trigger at LHC

Pascal Dupieux
LPC Clermont-Fd, IN2P3/CNRS and Univ. Blaise Pascal
63177 Aubière cedex, France
Email: dupieux@clermont.in2p3.fr
for the ALICE Collaboration

***Abstract*— ALICE, the experiment dedicated to the study of heavy ion collisions at LHC, will be equipped with a forward spectrometer to identify heavy quarkonium states of the J/ψ and Υ family from their decay into muons. The trigger system of the spectrometer consists of four planes of resistive plate chambers, front-end and fast-decision electronics. It is designed to reconstruct muon tracks in a large background environment in order to provide a fast trigger signal to the spectrometer. Results from tests of a trigger prototype that have been carried out with the muon beam of the CERN/SPS at the Gamma Irradiation Facility (GIF) will be presented. The (muon) track-finding efficiency as well as the robustness of the system to the uncorrelated background induced on the detector by the GIF source are discussed. Special emphasis is put on the timing aspects which are crucial at LHC owing to the 25 ns interval between the bunch crossings.**

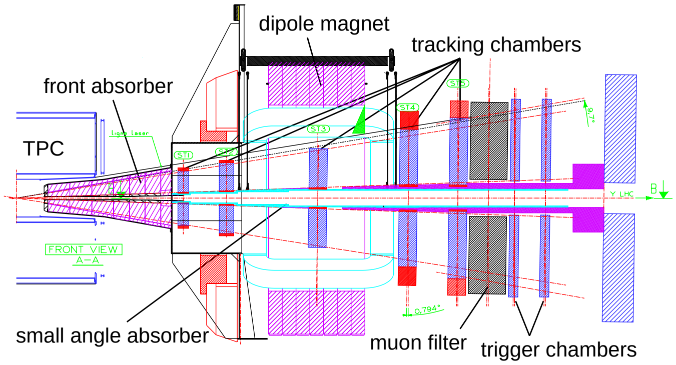

Fig. 1. Sketch of the ALICE muon spectrometer.

I. INTRODUCTION

ALICE[1] (A large Ion Collider Experiment) will be the only detector dedicated to the study of nucleus-nucleus collisions at the LHC. Its physics program aims at investigating the properties of strongly interacting matter at extreme energy density where the formation of the Quark Gluon Plasma (QGP) is expected. Among the most promising probes of the QGP, heavy quarkonium states provide, via their dimuon or dielectron decays, essential information from the earliest and hottest stages of the collisions (for reviews, see [2], [3]).

In ALICE, dimuon measurements will be performed by means of a forward spectrometer[4] which is designed to identify the full set of quarkonium resonances from the ϕ to the Υ, with high statistics and high resolution. This spectrometer (Fig. 1) consists in a front absorber, a small angle absorber (beam shielding), a large dipole magnet, ten high granularity tracking chambers, a muon filter and a trigger system.

This system is described in the next section, with particular emphasis on the trigger electronics. The performances of a reduced-size prototype, called the ”mini-trigger”, have been investigated during a test performed at the GIF (Gamma Irradiation Facility[5]) at CERN and are discussed in what follows.

A. The trigger system of the muon spectrometer

The dimuon trigger is involved in the level 0 of ALICE general trigger system. The trigger signal must be delivered in less than 1.2 μs to the detectors that require it. A Higher level of trigger, not described in this note, implemented in computer farms is also foreseen.

The system is based on two large area (30m^2) detector stations MT1 and MT2, located 16m and 17m away from the interaction center, outside the dipole magnet. A station consists in two planes of 18 RPC (Resistive Plate Chamber) each. The RPC are operated in streamer mode. They are read-out in X and Y directions with strips equipped with a dedicated front-end electronics (FEE). The FEE uses the ADULT (A DUaL Threshold[6]) ASIC, developped by the group of micro-electronics of LPC Clermont-Fd. This ASIC allows to improve significantly the time resolution of RPCs in streamer mode. Typical values of $\sigma_t < 2$ ns are reached, regardless of the detector running voltage, with a skew of about 3 ns/kV.

The signals from the FEE, the X and Y fired strip pattern of the four detection planes, are sent to the Local trigger electronics, which is housed in VME 9U boards and based on FPGA (Field Programmable Gate Array) circuits. Each Local board receives 128 signals from the FEE. The whole trigger system is divided in 234 detection areas, each of them being associated with a Local trigger board.

Single (muon) tracks are reconstructed following the algorithms, L0-X in the bending plane of the dipole and L0-Y in the other direction, implemented in the FPGAs of each Local board. The L0-X and L0-Y algorithms require 3/4 (4/4 also implemented) detector planes fired to validate a track. The magnetic deviation (track angle between the two trigger stations, with respect to the line aiming at the interaction

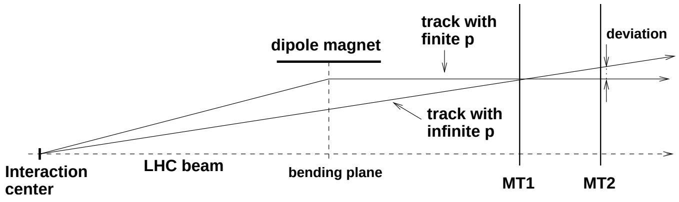

Fig. 2. Principle of the deviation measurement with the trigger system.

center, as shown in Fig. 2) is also roughly estimated by the L0-X algorithm. A cut on the measured deviation can be performed, by means of a Look-up-Table implemented in the Local board, in order to reject low transverse momentum muons which originate, to a large extent, from pion and kaon decay. Other functions like programmable masks of the inputs and DaQ interface are also implemented.

The response time of the Local boards is 250 ns. The dimuon trigger signal is issued, by combining two like-sign or unlike-sign tracks over the whole setup.

B. Setup of the mini-trigger

The test has been carried out with the 120 GeV/c SPS muon beam. The intense photon flux of the GIF induces a non-correlated background on the detectors. At the setup location, the maximum background rate is 320(110) $\mathrm{Hz/cm}^2$ on the detector close to (far from) the source. The background rate can be varied by means of absorbers.

The setup (Fig. 3) consists in four $50 \times 50~\mathrm{cm}^2$ RPC planes, geometrically spaced like in ALICE, perpendicular to the beam. Two $30 \times 30~\mathrm{cm}^2$ scintillator hodoscopes are placed upstream and downstream the RPCs.

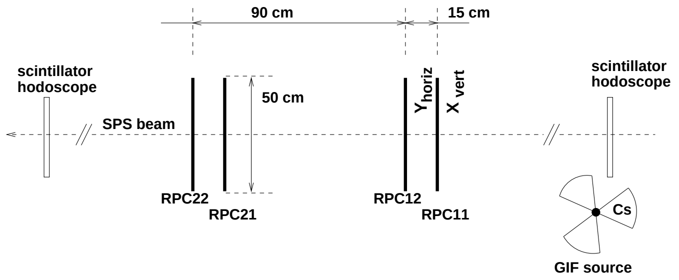

Fig. 3. Sketch of the experimental setup of the mini-trigger experiment.

Each RPC is readout on both sides of the gas gap by 16 X-Y orthogonal strips, equipped with ADULT front-end electronics. The length and width of the strips are 50 cm and 2 cm, respectively. The X-Y pattern of the fired strips is transmitted to a single Local trigger board, in LVDS differential mode, along 25 m long cables. Here the signals are latched and sampled at the 40 MHz clock frequency and the trigger algorithm is executed. The fired strip pattern as well as the response at different stages of the algorithm are stored in the DaQ pipeline of the Local trigger board.

The data in the DaQ pipeline are frozen and then readout on occurrence of a trigger signal. The trigger may be delivered by:

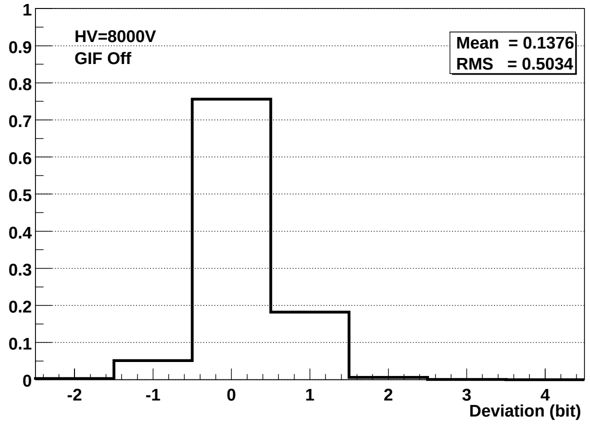

Fig. 4. Track deviation spectrum, in bit unit, given by the Local trigger algorithm, for a RPC running voltage of 8kV with GIF off. One bit corresponds roughly to the half width of a strip, thanks to the declustering algorithm performed in the Local board. The fraction of events with a given deviation is indicated by the vertical scale.

- the scintillator hodoscopes, when a muon from the beam is detected. Note that the hodoscopes are protected from the GIF background. Such a trigger is used for the determination of the track-finding efficiency of the mini-trigger. The track deviation measured by the mini-trigger is close to zero (Fig. 4) since the beam direction is orthogonal to the setup. Note that the alignment accuracy between strips of the four detector planes was not better than a few millimeters in this test, which may explain the asymmetry of the track deviation spectrum. The accuracy of the measured deviation can be roughly translated, in ALICE conditions, into a transverse momentum pt resolution of 10 %, at pt=1 GeV/c (typical cut). Of course, no cut on the deviation is performed here (by means of the Look-Up-Table in the Local trigger board) for track-finding efficiency measurements;
- the Local trigger board itself, after the trigger algorithm is executed. This actually corresponds to the standard running mode in ALICE. The track-finding efficiency is 100% by definition in this case. The rates of this trigger at various background levels, with beam off, give useful information about the robustness of the setup against uncorrelated background.

Very important, the beam muons which are synchronous with the clock (within $\sim \pm$ 2.5 ns) are previously selected by means of a dedicated electronic device.

C. Performances of the mini-trigger

1) RPC efficiency: The RPC efficiency is obviously a key feature for the track-finding efficiency of the mini-trigger. RPC efficiency curves measured with GIF off are shown in Fig. 5 for X-planes of the four detectors. Comparable efficiencies (not shown) are achieved for the Y-planes and also with GIF on. The four RPCs exhibit a very homogeneous response with a knee at around 7.6 kV followed by a wide plateau reaching 98% efficiency.

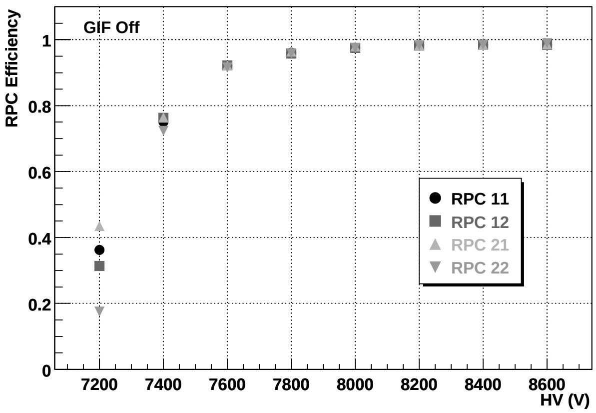

Fig. 5. RPC efficiency (X-planes) versus the applied voltage with GIF off. The normalisation of the efficiency is provided by the scintillator hodoscope.

2) Track-finding efficiency vs. RPC running voltage: The track-finding efficiency of the mini-trigger, vs. the RPC running voltage and for different background rates, is shown in Fig. 6 and Fig. 7 for the 3/4 and 4/4 coincidence requirement, respectively. As expected, the track-finding efficiency exhibits a shape similar to that of the RPC efficiency. No effect of the background can be evidenced.

However, the knee and the amplitude of the plateau depends on the coincidence requirement. Indeed, i) with the 4/4 coincidence requirement, the knee is moved towards higher voltages and ii) the plateau reaches 98% and 94% efficiency with the 3/4 and the 4/4 coincidence requirement, respectively.

A closer look at the data indicates that there are correlations between the RPC inefficiencies which are attributed to a partial geometrical overlap of the RPC spacers in the different detection planes, with respect to the beam direction. These correlations explain a large part of the track-finding efficiency loss with the 3/4 coincidence requirement. Indeed, with independent 98% RPC efficiencies, almost 100% track-finding efficiency would be expected with the 3/4 coincidence requirement. Such geometrical overlap of the spacers should be avoided to a large extent in ALICE thanks to the different geometry of the setup. Note that, on the other hand, this effect contributes to increase a little bit the track-finding efficiency, as compared to expectations with independent RPC efficiencies, with the 4/4 coincidence requirement.

Anyhow these experimental results demonstrate clearly that the track-finding efficiency is better with the 3/4 than with the 4/4 coincidence requirement, while the robustness of the system to uncorrelated background is still satisfactory.

3) Track-finding efficiency vs. clock phase: The clock phase must be optimised to latch the signal from the FEE with the goal of maximizing the track-finding efficiency. The track-finding efficiency vs. the clock phase is shown in Fig. 8, for GIF off (top) and GIF on (bottom), with the 3/4 coincidence requirement. A $\sim$10 ns wide plateau at 98 % efficiency is reached for RPC running voltages greater than 7600 V (HV=7600 V corresponds to the efficiency knee of the detectors). It demonstrates that, despite all sources of timing dispersion, a sufficient safety margin is left for the timing optimisation.

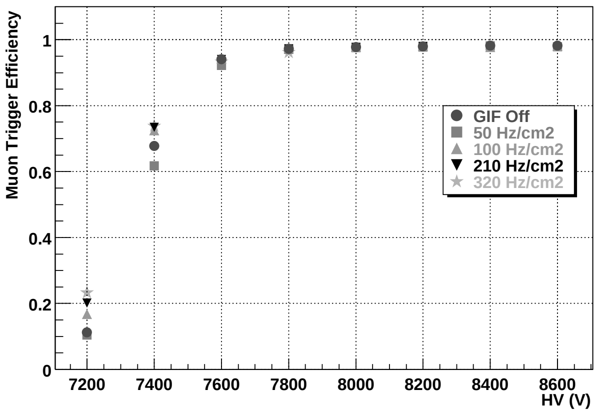

Fig. 6. Track-finding efficiency with the 3/4 coincidence requirement vs. the RPC running voltage, for different background rates (indicated for RPC11).

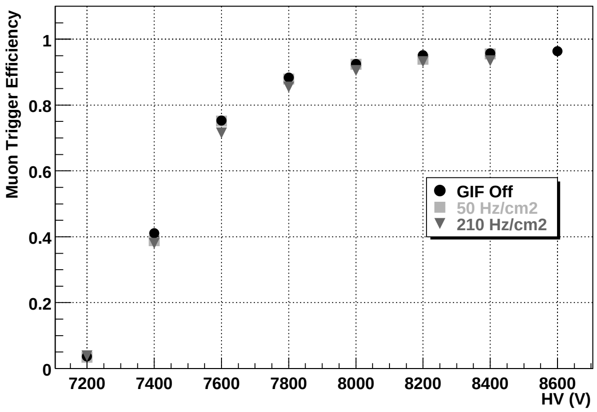

Fig. 7. Track-finding efficiency with the 4/4 coincidence requirement vs. the RPC running voltage, for different background rates (indicated for RPC11).

4) Timing optimisation and monitoring in ALICE: Within the mini-trigger experiment, the optimal clock phase is found easily thanks to the reference provided by the scintillator hodoscopes. It is shown in Fig. 9 that the best clock phase can also be determined self-consistently, without external reference, by computing the ratio of the trigger yields with the 4/4 over the 3/4 coincidence requirement. The values of this ratio are peaked at the optimal clock phase setting and are moreover correlated with the value of the track-finding efficiency itself. This looks very promising and will be available for each Local trigger board in ALICE.

5) Robustness to uncorrelated background: The trigger rate delivered by the Local board itself with the 3/4 coincidence requirement, beam off, is of the order of 3 per minute at the maximum background. This is in agreement with simple estimates of the expected event count created by an uncorrelated

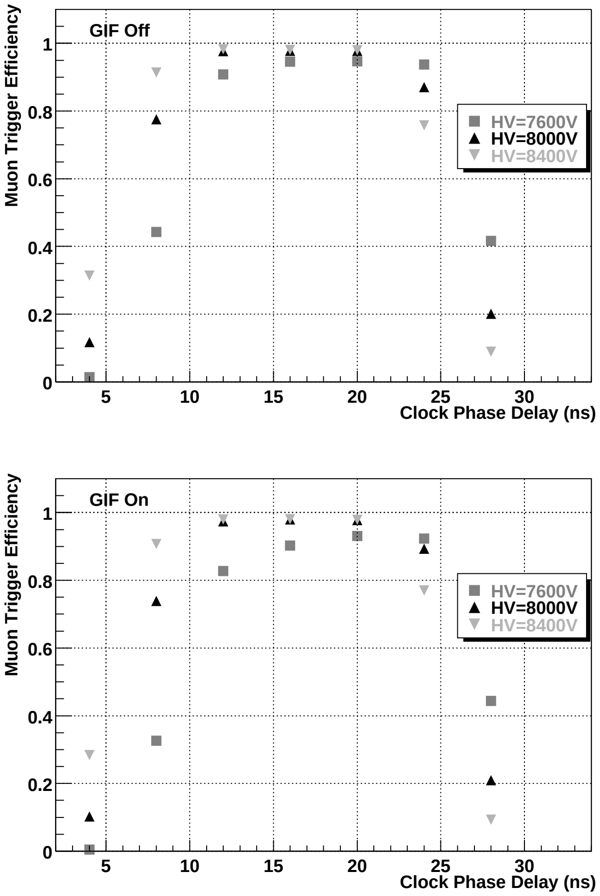

Fig. 8. Track-finding efficiency with the 3/4 coincidence requirement vs. the clock phase, for different RPC running voltages with GIF off (top) and GIF on (bottom, corresponding to 210 Hz/cm^2 on RPC11).

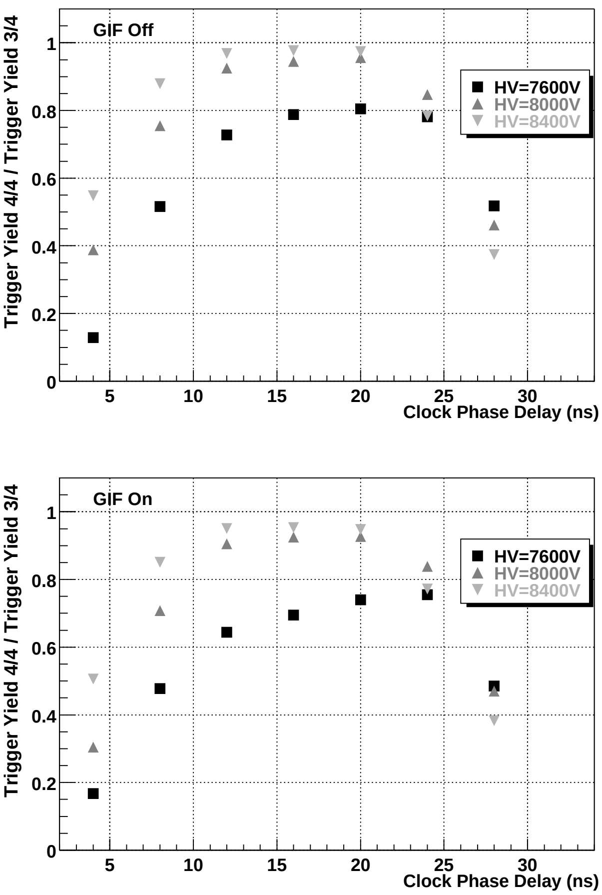

Fig. 9. Ratio of the Local trigger yield with the 4/4 over the 3/4 coincidence requirement vs. the clock phase, for different RPC running voltages with GIF off (top) and GIF on (bottom, corresponding to 210 Hz/cm^2 on RPC11).

background such as the one at the GIF. The extrapolation of this result to ALICE conditions is however not straightforward because, at LHC, the background is expected to be more complex and time-correlated with the signal. Detailed simulations were required to evaluate the expected trigger rate in ALICE. The results of these simulations are given in [4].

II. CONCLUSION

The ALICE muon spectrometer will need a high-performance trigger to select the quarkonium states in heavy ion collisions at LHC. The performances of a small scale prototype including most of the final equipments developed for the ALICE muon trigger have been investigated in detail. It is found that the RPC detector efficiency as well as the mini-trigger track-finding efficiency reach a 98 % plateau, regardless of the background rate, up to 320 Hz/cm^2. The timing quality of the detector associated with its ADULT front-end electronics is responsible for this excellent result. A deep investigation of the timing aspects has also demonstrated that, despite all sources of timing dispersion, a good safety margin is left on the timing optimisation. It is shown that this optimisation can be performed self-consistently, without any external reference, from the calculation of the ratio of the trigger yields with the 4/4 over the 3/4 coincidence requirement. This method should be simple and powerful to perform the time tuning in ALICE. Finally, the robustness of the muon trigger algorithm against a high uncorrelated background has been established eventhough this result cannot be extrapolated straightforwardly to running conditions in ALICE.

All these findings are an encouraging step toward the construction phase of the ALICE muon trigger.

REFERENCES

[1] ALICE Collab., ALICE Technical Proposal, CERN/LHCC 95-71 (1995).
[2] H. Satz, Rept. Prog. Phys. 63 (2000) 1511.
[3] R. Vogt, Phys. Rept. 310 (1999) 197.
[4] ALICE Collab., Technical Design Report, CERN/LHCC 99-22 (1999); ALICE Collab., Addendum to the Technical Design Report, CERN/LHCC 00-46 (2000).
[5] S. Agosteo et al., Nucl. Instrum. Meth. A 452 (2000) 94.
[6] R. Arnaldi et al, Nucl. Instrum. Meth. A 457 (2001) 117; P. Dupieux et al., Nucl. Instrum. Meth. A13586, (in press).